Tellus (2001), 53B, 260–272
Printed in UK. All rights reserved

TELLUS
ISSN 0280–6509

Mechanisms of sulphate aerosol production in clouds: effect of cloud characteristics and season in the Indian region

By CHANDRA VENKATARAMAN[1], ANURAG MEHRA[2] and PRASHANT MHASKAR[2], [1]*Centre for Environmental Science and Engineering;* [2]*Department of Chemical Engineering, Indian Institute of Technology, Bombay, Powai, Mumbai, 400 076, India*

(Manuscript received 27 May 1999; in final form 15 October 2000)

ABSTRACT

Measurements made during the Indian Ocean Experiment (INDOEX) in 1998, indicate likely regional atmospheric effects of sulphate aerosol over India including the potential for cloud processing of SO_2 to sulphate. Sulphate aerosol production in clouds was examined for cloud characteristics and pollutant concentrations typical of the Indian region, to assess the contribution of different mechanisms to sulphate formation. A simple model was formulated incorporating gas-liquid equilibria, gas-phase mass transfer, SO_2 oxidation in the gas phase by OH· radicals and in the aqueous phase by H_2O_2, O_3 and O_2 catalysed by Fe^{3+} and Mn^{2+} in a cloud with uniformly sized drops. Sulphate formation was simulated in St/Sc, Cu and Cb clouds using an initial pH of 6.5, likely to occur in this region, for cloud drop diameters of 10, 50 and 100 μm. The clouds were assumed to have nucleated on ammonium sulphate aerosols and contained reported background concentrations of these ions in clean rainwater over the Indian ocean. The simulations produced final cloud pHs of 4.5–5 and final sulphate concentrations of 25–90 μM, in agreement with the range of reported preliminary measurements. An examination of mass transfer effects showed that the characteristic diffusion times of H_2O_2 and SO_2 were lower by a factor of 10 or more than the respective reaction times, indicating that mass transfer effects would not limit the rate of S_{VI} formation under likely atmospheric conditions. Sulphate formation in St/Sc clouds was shown to likely be SO_2 limited in July and H_2O_2 limited in January. In all cases, the gas phase reaction and the O_2 reaction catalysed by Mn^{2+} and Fe^{3+} contributed less than 1% to the S_{VI} produced. In St/Sc and Cu clouds, 85–96% of the S_{VI} was from the H_2O_2 reaction. In Cb clouds about 60–75% of the S_{VI} was from the H_2O_2 reaction and 25–41% from the O_3 reaction. In Cb clouds, the short residence and the persistence of alkaline conditions in the earlier part of the cloud cycle, enhance the contribution of the O_3 reaction to the greatest extent. If alkaline conditions were to persist throughout the cloud cycle (from cation chemistry not simulated in this model), the contribution of the O_3 reaction to S_{VI} could be further enhanced.

1. Introduction

The strong regional variation in climate forcing by anthropogenic sulphate aerosols has been recently recognized. The direct effect, from solar radiation scattering by sulphate particles, reduces net irradiance at the ground by -0.3 to -1 Wm^{-2} (Charlson et al., 1991; Kiehl and Briegleb, 1993; Kiehl and Rodhe, 1995; Boucher and Anderson, 1995). The indirect effect, in which aerosols act as cloud condensation nuclei (CCN) and alter the structure and reflectivity of clouds, is similar in magnitude to the direct effect, but has a large

* Corresponding author.
e-mail: chandra@cc.iitb.ernet.in

uncertainty associated with it (Boucher et al., 1995). Potential regional atmospheric effects of sulphate aerosols include modification of clouds, precipitation and the radiation balance (Charlson et al., 1987; Hobbs, 1993; Boucher et al., 1995). GCM estimates of sulphate indirect forcing indicate a magnitude of -0.6 to -1 Wm^{-2} averaged over the Northern hemisphere (Boucher et al., 1995) and a correlation between sulphate concentration, CCN and cloud albedo (Boucher and Lohmann, 1995). A decrease in precipitation over India and south-east Asia was predicted using prescribed future sulphate aerosol concentrations in GCM simulations (Boucher et al., 1998).

Tropospheric sulphate aerosol is formed from SO_2 oxidation in the gas phase and in aqueous phase in cloud drops. The aqueous phase reactions have been estimated to contribute over two-thirds of the sulphate yield in general circulation model simulations of the global sulphur cycle (Pham et al., 1995; Chin et al., 1995; Feichter et al., 1996). The conversion was seen to depend upon reactant and oxidant concentrations, cloud pH, temperature and cloud liquid water content, all of which vary with season and region over small scales (even within a cloud). Simulated sulphate formation was oxidant or SO_2 limited based on variations in these parameters (Langner and Rodhe, 1991; Feichter et al., 1996).

To examine the relative importance of aqueous reactions contributing to sulphate formation, Pandis and Seinfeld (1989) performed a sensitivity analysis of a system incorporating gas-phase and interfacial mass transfer, and a condensed chemical mechanisms of 109 aqueous phase reactions and 37 equilibrium reactions. Aqueous phase oxidation of SO_2 by $H_2O_2^{aq}$ was the dominant reaction and primary contributor to sulphate formation. Cloud water pH determined the extent of solubility of SO_2 and its availability for aqueous conversion to sulphate. Reactions which were sources or sinks for $H_2O_2^{aq}$, and aqueous reactions with oxidants like O_3, O_2 (catalysed by Fe^{3+} and Mn^{2+}), OH^- and HSO_3^- affected sulphate formation to a smaller extent.

Cloud microphysics has been shown to have a significant effect on the chemistry of SO_2 to sulphate conversion in clouds (Hegg and Larson, 1990; Gurciullo and Pandis, 1997; Kreidenweis et al., 1997; Zhang et al., 1999). Explicit microphysical treatment resulted in higher predicted sulphate formation, from the size-dependence of pH and reaction rates not accounted for in bulk chemistry models. The magnitude of sulphate underprediction by the bulk models was found significant under low H_2O_2 concentrations (less than 0.5 ppbv) likely to occur in winter, but not significant under high NH_3 concentrations. The H_2O_2 reaction, being pH insensitive, added sulphate evenly across the drop spectrum (Hegg and Larson, 1990; Kreidenweis et al., 1997) while the O_3 reaction added sulphate to the more alkaline drops. The initial aerosol spectrum and composition affected both the size-dependent sulphate production rates (Hegg et al., 1992; Kreidenweis et al., 1997) and the resulting droplet spectrum characteristics.

Recent INDOEX measurements indicate that sulphate is likely to play a significant role in precipitation and climate modification over India. Sulphate concentrations in Indian ocean aerosol were comparable to those in background continental aerosol (Kulshrestha et al., 1999; Momin et al., 1999). Aerosols and rainwater over the continent had high ammonium and calcium concentrations resulting in high alkalinity and leading to a pH of around 6–7.5 (Parashar et al., 1996). However, rainwater over the ocean was found acidic (pH from 4.2–6) with significantly elevated sulphate/sodium ratios compared to those in sea water, attributable to excess free acidity from sulphate (Kulshrestha et al., 1999). Sulphate concentrations in rainwater at background continental sites (Parashar et al., 1996) were similar to that over the pristine Indian ocean (Kulshrestha et al., 1999). However, rainwater collected during ship cruise near the continent, had elevated sulphate concentrations indicating cloud processing of SO_2 as its likely origin. Limited trace gas concentrations reported from the continent also indicated the potential for SO_2 cloud processing.

In the present study, our goal is to examine the importance of various mechanisms of sulphate formation under cloud and atmospheric conditions encountered in the Indian region. A simple model is formulated to simulate cloud chemistry (including alkalinity) and microphysical effects likely to occur in this region. The paucity in this region of comprehensive pollutant measurements dictates the need for a simple model. We have developed a model including gas phase mass

transfer, chemical equilibria and oxidation reactions of SO_2 in gas and aqueous phase. The competing processes for sulphur dioxide conversion include (i) gas-phase oxidation of SO_2 by $OH^{\cdot}$ radicals and mass transfer of product H_2SO_4 to cloud drops, (ii) gas-phase mass transfer of SO_2, O_3, H_2O_2 and NH_3 to cloud drops followed by aqueous phase reactions and (iii) gas phase oxidation followed by binary homogeneous nucleation of products to form new droplets. The extent of sulphate formation in three cloud types [Stratocumulus/Stratus (St/Sc), Cumulus (Cu), Cumulonimbus (Cb)] is simulated for typical January and July conditions.

2. Model description

We use a Lagrangian trajectory model of an air parcel rising through a cloud containing single sized drops whose number concentration is derived from the liquid water content (LWC) of the cloud type. A constant updraft velocity and cloud residence time are assumed, based on the cloud type. During passage of the parcel through cloud, gas-liquid mass transfer, gas-phase and aqueous-phase reactions occur. Concentrations of gas-phase reactants (SO_2, H_2O_2 and O_3) decrease and aqueous-phase products increase during the simulation with increasing cloud residence time. Gas phase diffusion is explicitly treated, while the aqueous phase is assumed to be uniformly mixed, a reasonable assumption for cloud drops smaller than 100 μm diameter (Schwartz, 1986).

The inter-phase mass transfer of gas phase species and their equilibrium with aqueous phase species is described by mass balance equations of the form:

$$\frac{\mathrm{d}C_i^{\mathrm{aq}}}{\mathrm{d}t} = k_i^{\mathrm{g}} A_{d_{\mathrm{p}}} (C_i^{\mathrm{a}} - C_i^{\mathrm{g}}) - C_i^{\mathrm{g}} K_{\mathrm{H}i} \sum_j k_j, \qquad (1)$$

where C_i^{a} (atm) is the gas phase concentration of species i, C_i^{g} (atm) is the concentration at the gas-liquid interface of the cloud drop, C_i^{aq} (M) is the aqueous phase concentration, k_i^{g} (kmol $\mathrm{m}^{-2}\,\mathrm{s}^{-1}\,\mathrm{atm}^{-1}$) is the mass transfer coefficient and $K_{\mathrm{H}i}$ (M atm^{-1}) is the effective Henry's Law constant of species i. The pseudo first order reaction rate constants, k_j (s^{-1}) account for the aqueous phase oxidation by the oxidants ozone, hydrogen peroxide and oxygen.

For mass transfer from the air stream to the cloud drop with a relative updraft velocity V (m s^{-1}), the mass transfer coefficient is in the form to a freely falling drop (Bird et al., 1960):

$$k_i^{\mathrm{g}} = cD_i^{\mathrm{g}} \left[2 + 0.60 \left(\frac{d_{\mathrm{p}} V \rho}{\mu} \right)^{1/2} \left(\frac{\mu}{\rho D_i^{\mathrm{g}}} \right)^{1/3} \right] \Big/ d_{\mathrm{p}}, \qquad (2)$$

where D_i^{g} is the species diffusivity in air (a value of $1.26 \times 10^{-5}\,\mathrm{m}^2\,\mathrm{s}^{-1}$ has been used for all gas-phase species) and d_{p} the drop diameter (m). Cloud drop diameters are of the order of 10 μm or larger and the Knudsen number (ratio of mean free path of air to the the droplet radius) is much smaller than unity. Also, the sticking coefficient for SO_2 onto aqueous solutions is of the order of 0.01 (Schwartz, 1986), implying that interfacial mass transfer would not be rate limiting. Both these conditions result in a free molecular correction coefficient near unity, obviating the need for its use.

Gas phase species (SO_2, H_2O_2 and O_3) partition into aqueous phase governed by a temperature dependent Henry's Law constant (Table 1). Aqueous phase sulphur species are grouped into S_{IV} and S_{VI} whose concentrations (in mol/l of water) is given as:

$$[\mathrm{S_{IV}}] = [\mathrm{SO_2 \cdot H_2O}] + [\mathrm{HSO_3^-}] + [\mathrm{SO_3^{2-}}],$$

$$[\mathrm{S_{VI}}] = [\mathrm{H_2SO_4^{aq}}] + [\mathrm{HSO_4^-}] + [\mathrm{SO_4^{2-}}].$$

For species that undergo ionic dissociation, an effective Henry's Law constant is used which contains all ionic forms. For example, SO_2 dissolution and ionisation to give three aqueous phase species ($SO_2 \cdot H_2O$, HSO_3^- and SO_3^{2-}) is governed by:

$$K_{\mathrm{H},S_{\mathrm{IV}}} = H_{S_{\mathrm{IV}}} \left(1 + \frac{K_{\mathrm{S1}}}{[\mathrm{H^+}]} + \frac{K_{\mathrm{S1}} K_{\mathrm{S2}}}{[\mathrm{H^+}]^2} \right), \qquad (3)$$

where K_{S1} and K_{S2} are the first and second ionic dissociation constants for $SO_2 \cdot H_2O$ (Table 1). S_{VI} ionisation into the species HSO_4^-, SO_4^{2-} and H_2SO_4 is governed by equilibrium reactions listed in Table 1.

The included gas and aqueous-phase reactions are listed in Table 2. Aqueous phase reactions include those of S_{IV} with H_2O_2, O_3 and O_2 (catalysed by Fe^{3+} and Mn^{2+}). These were chosen because they were identified as the important reactions by a previous sensitivity analysis of a

Table 1. *Equilibrium reactions and temperature dependent constants*

Reaction	Rate constant K_{298}	$-\Delta H/R$ (K)	Ref.
$SO_2 \rightleftharpoons SO_2 \cdot H_2O$	1.23 M atm^{-1}	3020	Smith and Martell (1976)
$SO_2 \cdot H_2O \rightleftharpoons HSO_3^- + H^+$	1.23×10^{-2} M	1960	Smith and Martell (1976)
$HSO_3^- \rightleftharpoons SO_3^{2-} + H^+$	6.61×10^{-8} M	1500	Smith and Martell (1976)
$H_2SO_4(aq) \rightleftharpoons HSO_4^- + H^+$	1000 M		Perrin (1982)
$HSO_4^- \rightleftharpoons SO_4^{2-} + H^+$	1.02×10^{-2} M	2720	Smith and Martell (1976)
$H_2O_2(g) \rightleftharpoons H_2O_2(aq)$	7.1×10^4 M atm^{-1}	6621	Martin and Damschen (1981)
$O_3(g) \rightleftharpoons O_3(aq)$	1.13×10^{-2} M atm^{-1}	2300	Kosak-Channing and Helz (1983)
$NH_3(g) \rightleftharpoons NH_3 \cdot H_2O$	62 M atm^{-1}		Seinfeld and Pandis (1998)
$NH_3 \cdot H_2O \rightleftharpoons NH_4^+(aq) + OH^-$	1.7×10^{-5} M		Seinfeld and Pandis (1998)

Table 2. *Gas and aqueous phase reactions, rate expressions and constants*

Reaction	Rate expression	Rate constant k_{298}	E/R (K)	Ref.
$SO_2 + OH \rightarrow H_2SO_4$	$k_{11}[OH^{\cdot}][SO_2^g]$	$k_{11} = 1500$ ppm^{-1} min^{-1}		Atkinson and Lloyd (1984)
$S(IV) + \frac{1}{2}O_2 \xrightarrow{Mn^{2+},Fe^{3+}} S(VI)$	$k_{21}[Fe^{3+}][Mn^{2+}][H^+]^{-0.74}$, pH $\leqslant 4.2$	$k_{21} = 8.1 \times 10^{19}$ M^{-1} s^{-1}	-8432	Ibusuki and Takeuchi (1987)
	$k_{22}[Fe^{3+}][Mn^{2+}][H^+]^{0.67}$, pH $\geqslant 4.2$	$k_{22} = 5.47 \times 10^{25}$ M^{-1} s^{-1}	-8432	
$S(IV) + O_3 \rightarrow S(VI) + O_2$	$\{k_{31}[SO_2 \cdot H_2O] + k_{32}[HSO_3^-] + k_{33}[SO_3^{-2}]\}[O_3^{aq}]$	$k_{31} = 2.4 \times 10^4$ M^{-1} s^{-1} $k_{32} = 3.7 \times 10^5$ M^{-1} s^{-1} $k_{33} = 1.5 \times 10^9$ M^{-1} s^{-1}	 -5530 -5280	Hoffman and Calvert (1985)
$S(IV) + H_2O_2 \rightarrow S(VI) + H_2O$	$k_{41}[H^+][H_2O_2^{aq}][HSO_3^-]/(1 + K_4[H^+])$	$k_{41} = 7.5 \times 10^7$ M^{-1} s^{-1} $K_4 = 13$ M^{-1}	-4430	Hoffman and Calvert (1985)

comprehensive aqueous phase chemical mechanism for cloud chemistry (Pandis and Seinfeld, 1989). Oxidation of SO_2 by $H_2O_2^{aq}$, which is pH independent for pH $\geqslant 2$, was the dominant reaction and the primary contributor to sulphate formation. The oxidation of S_{IV} by O_2 and O_3 are fairly strongly pH dependent and their contributions to sulphate formation varied with cloud pH. The rate expressions and rate constants for the H_2O_2 and O_3 reactions are given by Hoffmann and Calvert (1985) as summarised by Seinfeld and Pandis (1998). The O_2 rate equation is from Ibusuki and Takeuchi (1987), which accounts for Fe^{3+}/Mn^{2+} synergism and is valid over the entire pH range.

Gas phase SO_2 oxidation occurs by $OH^{\cdot}$ radicals, whose gas phase concentration is held constant, at 10^5 molec cm^{-3} throughout the simulation. The temporal variations in the gas phase species (for SO_2 and H_2O_2 and H_2SO_4) are given by equations of the form:

$$\frac{1}{RT}\frac{dC_i^a}{dt} = -A_{d_p}k_i^g(C_i^a - C_i^g)\mathrm{LWC} + k_j C_i^a/RT, \quad (4)$$

where A_{d_p} is the surface area of drops per unit volume of air (m^2 m^{-3}), k_i^g is the mass transfer coefficient (kmol m^{-2} s^{-1} atm^{-1}), k_j is the pseudo first-order rate constant for gas phase oxidation by $OH^{\cdot}$ radicals (s^{-1}), LWC (m^3 m^{-3}) is the liquid water content of the cloud, R is the universal gas constant (0.08206 atm M^{-1} K^{-1}) and T the drop temperature (K), assumed equal to the ambient cloud temperature.

An electroneutrality equation is used in which the bicarbonate ion concentration is fixed equal to that in unpolluted rainwater and held constant through the simulation. The initial sulphate concentration is prescribed, based on reported meas-

urements. The initial pH of the cloud is then prescribed by adjusting the ammonium ion concentration and the corresponding NH_3 gas-phase concentration. As the simulation proceeds, formation of S_{IV} and S_{VI} results in decreasing pH, which is calculated from the electroneutrality equation, in which $[H^+]$ is unknown:

$$[H^+] + [NH_4^+] = [HSO_3^-] + 2[SO_3^{2-}] + [HSO_4^-] + 2[SO_4^{2-}] + [OH^-] + [HCO_3^-]. \quad (5)$$

3. Input data

3.1. Cloud and atmospheric characteristics in the Indian region

We simulate sulphate formation in 3 types of liquid water clouds, stratus/stratocumulus (St/Sc), cumulus (Cu) and cumulonimbus (Cb). Cloud characteristics for 10–40 N (the extent of the Indian subcontinent) are taken from Lelieveld et al. (1989) who summarise zonal average cloud characteristics. The average cloud heights and updraft velocities (Table 3) result in average cloud residence times of about 12 min and 40 min, respectively, for Cb and Cu clouds. The average residence time in St/Sc is independent of cloud height and is approximately 40 min (Albrecht, 1989; Feingold et al., 1998). The initial temperature is taken as the cloud base temperature assumed as 15°C for winter (January) and 25°C for summer (July) conditions. A temperature profile of -6.6 C km^{-1} is assumed following the saturated lapse rate with air entrainment (Pruppacher and Klett, 1997).

Measurements made during the Indian Ocean Experiment (INDOEX) in 1998, have given preliminary data on aerosol and rainwater composition over India (Kulshrestha et al., 1999; Momin et al., 1999). Comparing continental and ocean aerosol composition showed an order of magnitude elevation in ammonium, magnesium and especially calcium ion concentrations, in the former, which contribute to its alkalinity (Kulshrestha et al., 1999; Momin et al., 1999) evidenced by pH values of 6–7.5 (Parashar et al., 1996). The high ammonium concentrations indicate likely elevated concentrations of NH_3 (possibly from the large cattle population), reported as 4.2 ppb at a continental background location (Rao et al., 1999).

Sulphate concentrations in rainwater at background continental sites ranged 20–40 μeq l^{-1} (Parashar et al., 1996) similar to that over the pristine Indian ocean (0–50 μeq l^{-1}) (Kulshrestha et al., 1999). The sulphate in rainwater at remote sites indicates that clouds had nucleated on aerosol containing sulphate (likely ammonium sulphate). Potential for cloud processing of SO_2 is indicated by trace gas concentrations, reported from the continent and during ocean cruises. These include SO_2 at 1.3 ppb and O_3 at 10–70 ppbv (Naja et al., 1999; Mandal et al., 1999). Earlier measurements of surface ozone and ozone profiles over the continent gave concentrations in the 1–100 ppb range (Khemani et al., 1995). Reported rainwater concentrations of catalyst ions are 10^{-7} M for Fe^{3+} and 10^{-8} M for Mn^{2+} (Kulshrestha et al., 1999).

In the absence of cloud-water composition data in this region, and based on the above review of typical atmospheric and rainwater composition, we assume an initial cloud pH of 6.5, likely to be representative in the Indian region. Initial S_{VI} concentration was prescribed at 25 μM in winter and 15 μM in summer, using the range measured in rainwater at remote sites (Parashar et al., 1996; Kulshrestha et al., 1999). This was prescribed by fixing SO_4^{2-} and HCO_3^- ion concentrations, and adjusting the NH_3 concentration and the corresponding NH_4^+ ion concentration to give an initial cloud pH of 6.5. This required an NH_3 concentration of 1.5 ppb for winter (January) conditions and of 1 ppb for summer (July) conditions. Cloud-water concentrations of Fe^{3+} and Mn^{2+} (which catalyse SO_2 oxidation by O_2) were both maintained at an average value of 10^{-7} M. Typical

Table 3. *Summary of cloud characteristics*[a]

Cloud type	LWC (g/m^3)	v (m/s)	$(Z_o - Z_b)$ (km)	Residence time (s)
Cb	1.0	5–10(5)[b]	1.6–6.3(3.8)	760
Cu	0.5	0.5–2(1)	1.8–3.0(2.4)	2400
St/Sc	0.3	0.005–0.5(0.05)	0.8–1.8(1.3)	2400[c]

[a] From Lelieveld et al. (1989).
[b] Numbers in parentheses are average values used in the simulations.
[c] St/Sc residence time is independent of cloud height.

January and July concentrations of SO_2 and oxidants were assumed from previously prescribed values in general circulation model (GCM) studies (Chin et al., 1996; Pham et al., 1995), at the surface and aloft over the Indian region. The assumed concentrations of reactants and oxidants for typical January and July conditions are summarised in Table 4.

4. Model performance

Model performance was evaluated to examine the ability of this simple model to reproduce results from more complex models which cannot be used in this instance because of the lack of measurements in this region, which are needed as inputs. We simulated the base case scenario for daytime north-eastern United States conditions used by Pandis and Seinfeld (1989) as well as data sets simulated by Seigneur and Saxena (1984) for urban fog and non-precipitating urban clouds in Los Angeles. Our simulation results agree within 4–8% of the base case results of Pandis and Seinfeld (1989) for aqueous S_{IV}, S_{VI} concentrations and pH. The agreement was less satisfactory (within 2–35% of final S_{VI} formed) with results of Seigneur and Saxena (1984) for cases of urban fog and urban non-precipitating clouds in Los Angeles. This disagreement is likely to result from the detailed gas-phase chemistry included in their model but omitted in our model, which would affect droplet-phase pH and the resulting sulphate formation rates. However, our model satisfactorily simulates the contribution of the various gas- and aqueous-phase reactions to sulphate formation for the cases examined. It can therefore be used with confidence to examine the importance of the various mechanisms of sulphate formation.

Table 4. *Concentrations of SO_2 and oxidants used in the model*

Chemical species	January	July
SO_2(ppb)	0.5–1.5(1)[a]	0.05–0.5(0.225)
O_3(ppb)	1–100(50)	1–100(50)
H_2O_2(ppb)	0.2–1.0(0.6)	1–1.5(1.25)
NH_3(ppb)	1.5	1
initial S_{VI}(μM)	25	15

[a] Numbers in parentheses are average values used in the simulations.

5. Results

5.1. *Effect of cloud drop size on sulphate formation*

In order to examine mass transfer effects on sulphate formation rate, we simulated drops of diameter, 10, 50 and 100 μm in St/Sc clouds, which have the lowest updraft velocities, resulting in the lowest mass transfer coefficients and the largest possible mass transfer effects (Figs. 1a–c). Figs. 1a, b show the time-varying concentrations of $H_2O_2^{aq}$ and S_{IV}. The steady-state $H_2O_2^{aq}$ concentration is reached later in larger drops (1 s in 10 μm drops versus 100 s in 100 μm drops). The

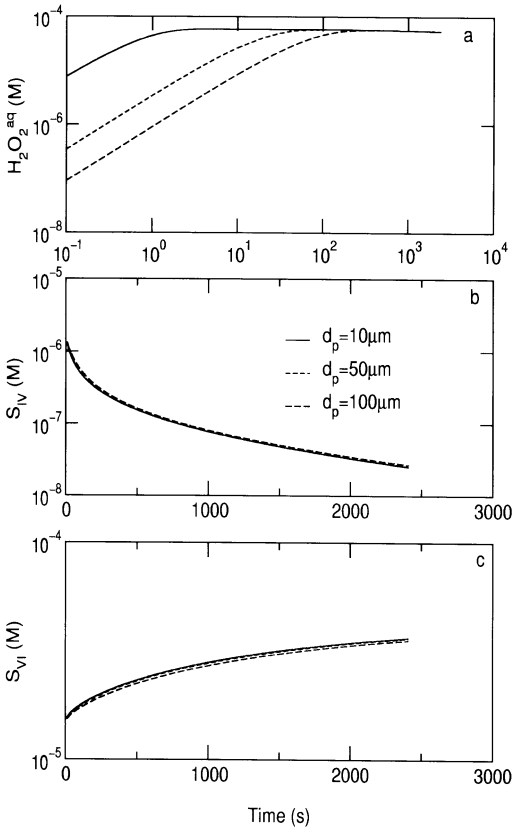

Fig. 1. Concentrations of aqueous phase species, (a) $H_2O_2^{aq}$, (b) S_{IV} and (c) S_{VI}, in cloud drops during an St/Sc cloud cycle for cloud-drop diameters d_p of 10, 50 and 100 μm.

high Henry's Law constant of H_2O_2 (Table 1) requires a large amount of H_2O_2 transfer to "fill up" the drop. The mass transfer coefficients, which depend upon drop diameter and updraft velocity, reduce by a factor of 9 with increase in drop diameter from 10 μm to 100 μm in a given cloud type. This results in the time lag to steady-state $H_2O_2^{aq}$ in larger drops. The final $H_2O_2^{aq}$ concentration, however, is the same in all cases indicating that it is in excess of reactive consumption. S_{IV} concentrations and pH drop sharply with the formation of S_{VI} and consequent increasing acidity in the drop.

The S_{VI} formed at the end of one cloud cycle of 40 min (Fig. 1c) varied within 1% for the different drop sizes indicating negligible mass transfer limitation to sulphate formation rates in drops up to 100 μm diameter. Measured cloud drop number size distributions show negligible numbers of drops larger than 80 μm diameter (Pruppacher and Klett, 1997) indicating that mass transfer of SO_2 and oxidants would not limit sulphate formation rates in most clouds.

Gas-phase species concentrations (Figs. 2a–c) show that the SO_2^g concentration drops at a constant rate (Fig. 2a). The $H_2O_2^g$ falls sharply during the initial time required for the drop to "fill-up" and remains constant beyond that because of negligible consumption by the aqueous-phase reaction (Fig. 2b). Gas-phase H_2SO_4 is formed from the gas-phase reaction of SO_2 with $OH^{\cdot}$ radicals and diffuses to the drops (Fig. 2c). There is an initial peak in the H_2SO_4 concentration followed by a decrease, as it diffuses to the drop. The rate of H_2SO_4 transfer to the drops depends upon the mass transfer coefficient, driving force and the interfacial drop surface-area. The mass transfer coefficient, as explained previously, reduces by a factor of 9 for the 100 μm drops compared to the 10 μm drops, and simultaneously the interfacial area reduces by a factor of 10, leading to an overall factor of 90 lower transfer rate of H_2SO_4 to the 100 μm drop. This results in a peak H_2SO_4 gas-phase concentration of the order of 3×10^{-5} ppb for $d_p = 100$ μm.

The characteristic diffusion time is given as the ratio of the Henry's Law constant to the mass transfer coefficient times the specific surface area of the drop. The characteristic reaction time (of S_{IV} oxidation by all oxidants) is given as the reciprocal of the product of the reaction rate

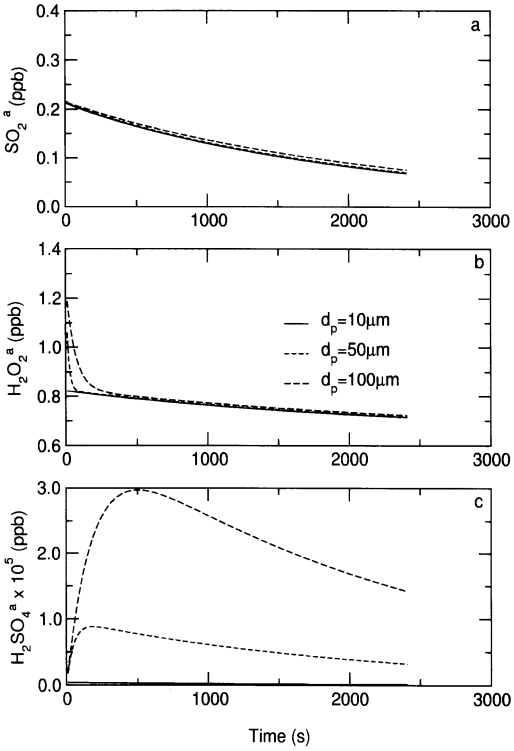

Fig. 2. Concentrations of gas phase species, (a) SO_2, (b) H_2O_2 and (c) H_2SO_4, in cloud air during an St/Sc cloud cycle for cloud-drop diameters d_p of 10, 50 and 100 μm.

constants (from Table 2) and appropriate aqueous phase oxidant concentrations. A comparison of these would establish the relative rates of diffusion and reaction processes. The diffusion and reaction times of SO_2 are both pH dependent because of the pH dependence of the SO_2 Henry's Law constant and reaction rate constants of the O_2 and O_3 reactions.

The SO_2 reaction and diffusion times are shown for drop diameters of 10 μm (Fig. 3a) and 100 μm (Fig. 3b) over the initial pH range of interest for January and July pollutant concentrations. For drops of 10 μm diameter, the reaction time is of the order 25 s for an initial pH of 5.0 and about 150 s for an initial pH of 6.0, indicating slower overall reaction rates at higher average alkalinity. However the diffusion times are of the order of 0.01 to 0.1 s, indicating faster diffusion than reaction for all cases considered. Even for the 100 μm drops (Fig. 3b), where the lower mass transfer

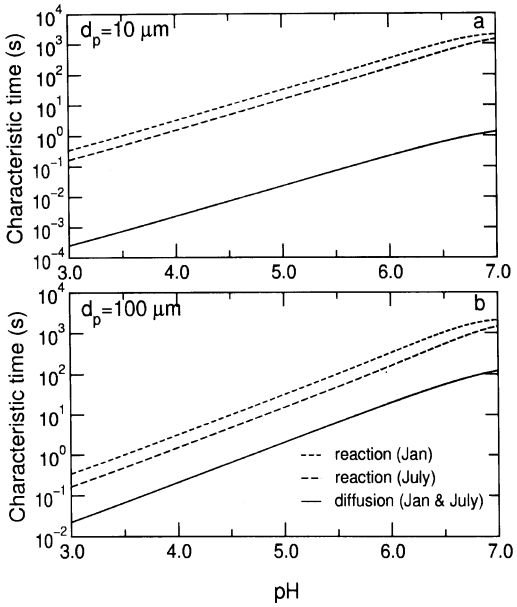

Fig. 3. Characteristic reaction and diffusion times for SO_2 as a function of initial cloud pH and drop diameter, for (a) 10 μm and (b) 100 μm drops.

coefficients result in longer diffusion times of 1–30 s, these are lower than corresponding reaction times for all cases. Therefore, the SO_2 diffusion rates would be faster than reaction rates for cloud conditions most frequently encountered. The unconsumed oxidants (H_2O_2 and O_3) remaining in droplet-phase would be released to the atmosphere at the end of the cloud cycle in the case of non-precipitating clouds.

We examined the rate of new particle nucleation from the gas-phase reaction product $H_2SO_4^g$ with water molecules, which has been suggested as potentially important in the mid-to-upper troposphere, in situations of low CCN concentrations and low temperatures (Kreidenweis et al., 1997). We used the nucleation rate suggested by Pandis et al. (1994) from hydrate theory for homogeneous binary nucleation multiplied by an experimentally determined nucleation factor. We assumed saturated conditions in the cloud (i.e., RH = 1) and the peak $H_2SO_4^g$ concentration of 2.9×10^{-5} ppb or 8.2×10^6 molecules cm^{-3} (Fig. 2c). A low nucleation rate of the order of 10^{-6} particles $cm^{-3}\,s^{-1}$ was obtained indicating negligible formation of new droplets even during the 40 min residence time in St/Sc clouds under these conditions. This may be enhanced by increase in the photolysis rate constant, of the gas-phase reaction, from the increase of actinic flux likely to occur within clouds because of multiple reflections by drops. The increase in the photolysis rate constant must be known to examine this effect further.

5.2. *Cloud pH effects*

Global average cloud pHs range from 4.5–5.5 (Seinfeld and Pandis, 1998), while those in the Indian region, based on measured rainwater pHs (Parashar et al., 1996; Kulshrestha et al., 1999) are likely to range 5.5–7.5. In the present model, the initial cloud pH is supplied and the pH at every time step during the cloud cycle calculated based on electroneutrality. While the H_2O_2 reaction is pH independent for pH $\geqslant 2$ (Pandis and Seinfeld, 1989), the O_2 and O_3 reactions are pH sensitive and likely to be significant under more alkaline conditions prevalent in the Indian region.

To determine the effect of pH on sulphate formation, we simulated initial pH's of 5.0 (global average) and 6.5 (typical Indian region) for Cb clouds in which these effects are likely to be most pronounced because of the low cloud residence times and the persistence of alkalinity in the early part of the cloud cycle. A drop diameter of 10 μm was taken for these simulations. The difference in the pH profile due to different initial pH diminishes rapidly within 100 s (Fig. 4a). However, the higher initial pH leads to an increase in the rate constant for O_3 reaction. There is also an increase in the effective Henry's constant for SO_2, resulting in greater S_{IV} availability as HSO_3^-. Both these conditions lead to the increased contribution of the O_3 reaction to sulphate formation at an initial pH of 6.5. At an initial pH of 6.5, of which about 74% is from the H_2O_2 reaction, 25% from the O_3 reaction and the remainder from the O_2 and gas-phase reactions (Fig. 5). For an initial pH of 5, over 86% of the S_{VI} formed was from the H_2O_2 reaction and about 13% from the O_3 reaction. In all cases, the O_2 reaction catalysed by Mn^{2+} and Fe^{3+} and gas-phase reaction contributed less than 1% of the S_{VI}. If alkaline conditions were to persist throughout the cloud cycle (from chemistry including Ca^{2+} and other cations, not simulated in this model), the contribution of the O_3 reaction to S_{VI} could be further enhanced.

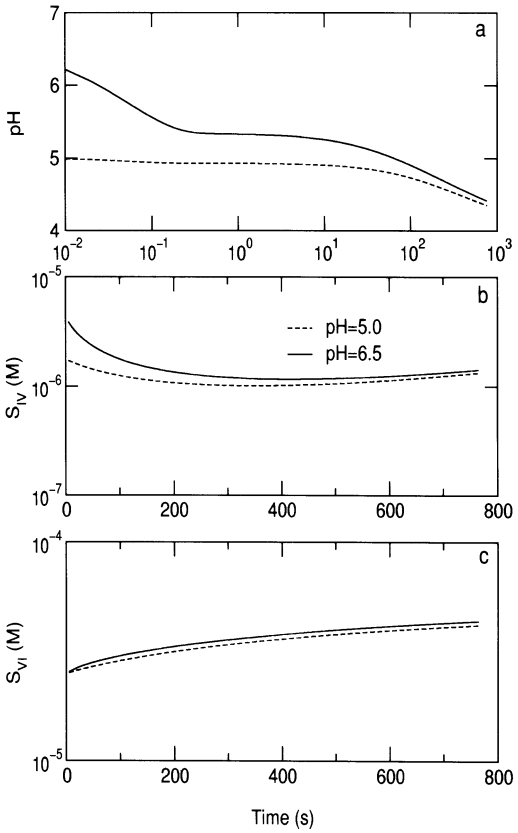

Fig. 4. Concentrations of aqueous phase species in Cb clouds in January for initial cloud pHs of 5.0 (global average) and 6.5 (Indian region average).

5.3. *Effect of cloud type*

Sulphate formation was simulated in the 3 different cloud types, St/Sc, Cu, Cb for an initial pH of 6.5 and a drop diameter of 10 μm. The difference in the liquid water content and cloud residence times for the three clouds affects the S_{VI} formation rates, contribution of the different reactions and the final S_{VI} concentrations. Comparing the contributions of the different reaction pathways to S_{VI} in the different clouds at initial pH 6.5 (Fig. 6), the conversion was primarily through the H_2O_2 reaction (85–96%) in St/Sc and Cu clouds, with the O_3 reaction contributing the remainder (4–15%) and negligible contributions from the O_2 and gas-phase reactions. In Cb clouds, however, the O_3 reaction has a significant contribution of 25–41%. Within the first 100s of the simulated

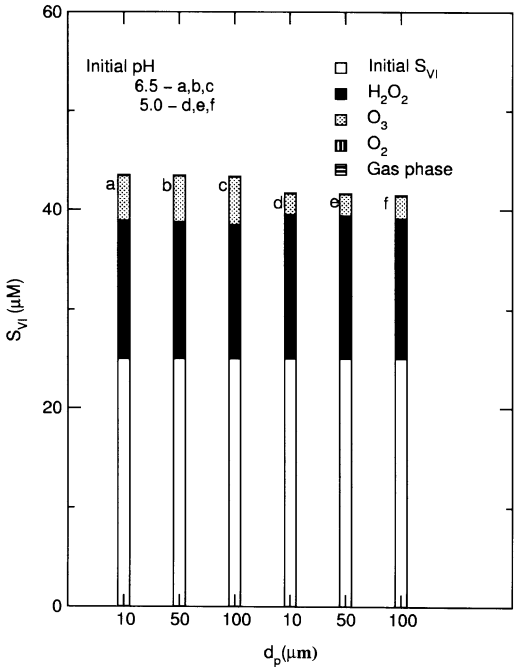

Fig. 5. Final concentrations of S_{VI} resulting from various reaction mechanisms in a Cb cloud for initial cloud pHs of 5.0 and 6.5 and varying drop diameters.

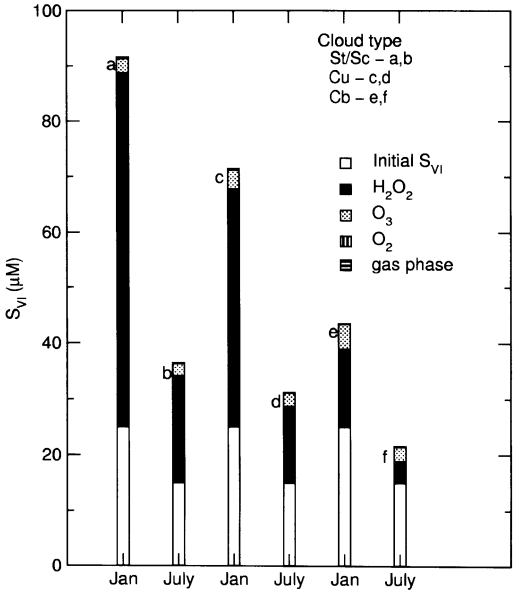

Fig. 6. Final S_{VI} concentrations in the three cloud types from different oxidation mechanisms for January and July conditions.

cloud cycle, the pH in all cloud types drops to lower than 5.2, where the H_2O_2 reaction would dominate.

St/Sc clouds were seen to have higher $H_2O_2^{aq}$ concentrations than the Cu and Cb clouds throughout the simulation. These resulted in high S_{IV} oxidation rates which, along with the long cloud residence times, resulted in the highest S_{VI} concentrations. While the largest amount of SO_2 was therefore processed in the St/Sc cloud in a single cycle, Cb clouds had the highest rate of SO_2 conversion. In all cases, the gas-phase reaction contributed to less than 0.2% of the S_{VI} formed.

5.4. *Effect of season*

Typical concentrations of SO_2 and oxidants in the Indian region (Table 4), reported in the literature, show higher SO_2 and lower H_2O_2 concentrations in January than July. We simulated an St/Sc cloud with d_p of 10 μm and initial pH of 6.5 to compare seasonal effects. In July, lower concentrations of SO_2 result in lower amounts of S_{IV} and lower concentrations of S_{VI} throughout the cloud cycle (Fig. 7). Because of the lower S_{IV} concentration, and high $H_2O_2^g$, excess $H_2O_2^{aq}$ accumulates without getting consumed during even the long cloud cycle of 40 min. In contrast, under January conditions, the high SO_2 and resulting S_{IV} concentrations result in the reactive consumption of $H_2O_2^{aq}$ and depletion of $H_2O_2^g$ about 10 min into the cloud cycle. Therefore, under January conditions sulphate formation in the St/Sc cloud would become H_2O_2 limited while under July conditions it would be SO_2 limited. In other cloud types, because of the smaller cloud residence time, none of the reactants are limiting during the course of a cloud cycle. In all cloud types, the final S_{VI} concentration is higher in January than in July (Fig. 6) with the highest concentration of 92 μm in the St/Sc cloud in January and lowest of 22 μm in a Cb cloud in July. However, these calculations are for a single cloud cycle and a cloud would typically undergo several such cycles in its lifetime.

This study has attempted to assess the importance of various mechanisms in sulphate formation over India, rather than build a complex model for simulating the system quantitatively. This approach was chosen in the absence of comprehensive measurements in the region needed for input and validation of complex models. The atmospheric data has been customised to Indian region and cloud characteristics taken for this latitude (Lelieveld et al., 1989), giving a complexity suitable to the goals of the study.

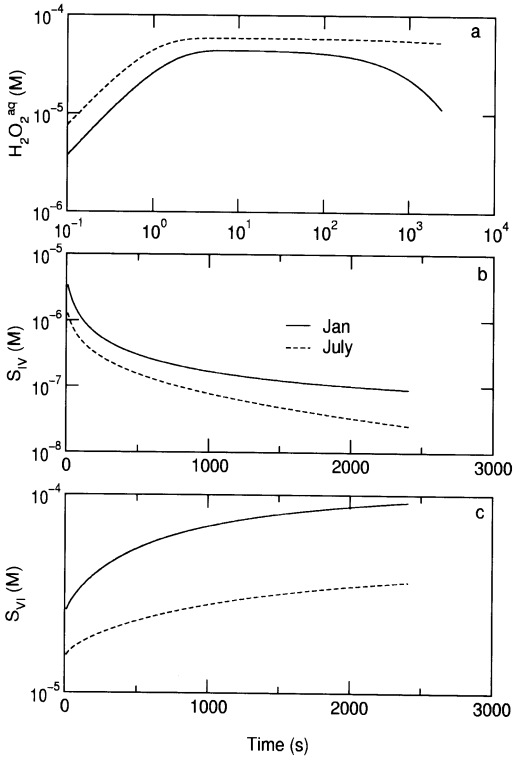

Fig. 7. Concentrations of aqueous phase species for January and July conditions in the Indian region in an St/Sc cloud.

6. Summary

Measurements made during the Indian Ocean Experiment (INDOEX) in 1998, indicate potential regional atmospheric effects of sulphate aerosol over India (Kulshrestha et al., 1999; Momin et al., 1999). While continental rainwater had a pH of around 6–7.5, rainwater over the ocean was found acidic (pH from 4.2–6) with significantly elevated sulphate/sodium ratios attributable to excess free acidity from sulphate. Rainwater collected during ship cruise through polluted plumes near the continent, had elevated sulphate concentrations compared to that in the clean Indian ocean,

indicating cloud processing of SO_2 as its likely origin. Limited trace gas concentrations reported from the continent also indicate the potential for SO_2 cloud processing.

Sulphate aerosol formation in clouds was examined for cloud characteristics and pollutant concentrations typical of the Indian region, to assess the contribution of different mechanisms to sulphate formation. A simple model was formulated incorporating gas-liquid equilibria, gas-phase mass transfer, SO_2 oxidation in the gas phase by $OH^{\cdot}$ radicals and in the aqueous phase by H_2O_2, O_3 and O_2 catalysed by Fe^{3+} and Mn^{2+} in a cloud with uniformly sized drops. The model was able to reproduce satisfactorily the contributions of the different reaction pathways for cases reported in the literature.

Sulphate formation was simulated in St/Sc, Cu, Cb clouds using an initial pH of 6.5, likely to occur in this region, for cloud drop diameters of 10, 50, 100 μm. The clouds were assumed to have nucleated on ammonium sulphate aerosols and contained reported background concentrations of these ions in clean rainwater over the Indian ocean. The simulations produced final cloud pHs of 4.5–5 and final sulphate concentrations of 25–90 μm. Reported rainwater pHs of 4.2–6.0 and sulphate concentrations of 25–200 μm (Kulshrestha et al., 1999) over the Indian ocean are likely from the cloud processing of SO_2, such as that simulated in this study.

Characteristic diffusion and reaction times were compared to examine possible mass transfer effects. The characteristic diffusion times of H_2O_2 and SO_2 were over a factor of 100 smaller than the respective reaction times for pH less than 7.0 and drop diameters smaller than 100 μm. This indicates that mass transfer effects would not limit the rate of S_{VI} formation under likely atmospheric conditions.

Formation of new droplets from binary homogeneous nucleation of gas-phase H_2SO_4 and water molecules was found to be negligible. A low nucleation rate of the order of 10^{-6} particles $cm^{-3}\,s^{-1}$ indicated negligible formation of new particles during even the long cloud residence time of 40 min in St/Sc clouds.

Under July conditions in St/Sc clouds, the low SO_2 and high H_2O_2 concentrations result in low S_{IV} dissolved in cloud and accumulation of the aqueous phase H_2O_2, which is not depleted by reaction. In contrast, under January conditions (high SO_2 and low H_2O_2 concentrations) H_2O_2 is consumed almost completely during a cloud cycle. Therefore, sulphate formation in St/Sc clouds would be SO_2 limited in July and H_2O_2 limited in January. In other cloud types, none of the reactants were limiting because of the smaller cloud residence times. The unused H_2O_2 would be liberated to gas phase on evaporation of non-precipitating clouds.

St/Sc clouds processed the largest amount of SO_2 and have the largest final S_{VI} concentrations. In all cases, the gas phase reaction and the O_2 reaction catalysed by Mn^{2+} and Fe^{3+} contributed less than 1% to the S_{VI} produced. In St/Sc and Cu clouds, 85–96% of the S_{VI} was from the H_2O_2 reaction. In Cb clouds about 60–75% of the S_{VI} was from the H_2O_2 reaction and 25–41% from the O_3 reaction. In Cb clouds, the short residence and the persistence of alkaline conditions in the earlier part of the cloud cycle, enhance the contribution of the O_3 reaction to the greatest extent. This reaction could contribute to significant sulphate formation in the monsoon season when Cb clouds would be most likely to occur. Also, continental aerosols in this region contain elevated magnesium and especially calcium ion concentrations. If alkaline conditions were to persist throughout the cloud cycle (from cation chemistry not simulated in this model), the contribution of the O_3 reaction to S_{VI} could be further enhanced.

7. Appendix

A_{d_p} specific drop surface area per volume of air ($m^2\,m^{-3}$)

C_i^{aq} concentration of species i in the aqueous phase (M)

C_i^a, C_i^g concentration of species i in the gas phase and the interface (atm)

K_{HS}, $H_{H_2O_2}$, H_{O_3} Henry's constant for SO_2, H_2O_2, O_3 ($M\,atm^{-1}$)

$H_2O_2^a$, O_3^a, SO_3^a, $H_2SO_4^a$ ambient concentrations of H_2O_2, O_3, SO_2, H_2SO_4 (atm)

$H_2O_2^g$, O_3^g, SO_2^g interfacial concentrations of H_2O_2, O_3, SO_2 (atm)

K_4, K_{S1}, K_{S2}, K_{S3}, K_{S4}

	equilibrium constants (M)
K_W	ionisation constant of water (M^2)
k_i^g	mass transfer coefficient of species i (kmol m^{-2} s^{-1} atm^{-1})
N_{d_p}	number concentration of drops with diameter d_p (m^{-3})
R	universal gas constant, 0.08206 atm M^{-1} K^{-1}
T	temperature (K)
S_{IV}	aqueous concentration of sulfur species in oxidation state +4 (M)
S_{VI}	aqueous concentration of sulfur species in oxidation state +6 (M)
d_p	drop diameter (m)
k_{21}, k_{22}, k_{31}, k_{32}, k_{33}, k_{41}	reaction rate constants (M^{-1} s^{-1})

REFERENCES

Barth, C. M., Hegg, D. A. and Hobbs P. V. 1992. Numerical modeling of cloud and precipitation chemistry associated with two rainbands and some comparisons with observations. *J. Geophys. Res.* **97(D5)**, 5825–4845.

Bird, R. B., Stewart, W. E. and Lightfoot, E. N. 1960. Interphase transport in multicomponent systems. In: *Transport phenomena*. Wiley, New York, pp. 636–676.

Boucher, O. and Anderson, T. L. 1995. GCM assessment of the sensitivity of direct climate forcing by anthropogenic sulfate aerosols to aerosol size and chemistry. *J. Geophys. Res.* **100(D9)**, 26,117–26,134.

Boucher, O., Le Treut, H. and Baker, M. B. 1995. Precipitation and radiation modelling in a general circulation model: interaction of cloud microphysical processes. *J. Geophys. Res.* **100(D8)**, 16,395–16,414.

Boucher, O. and Lohmann., U. 1995. The sulphate-CCN-cloud albedo effect. A sensitivity study with two general circulation models. *Tellus* **47B**, 281–300.

Boucher, O., Pham M. and Sadourny, R. 1998. General circulation model simulation of Indian summer monsoon with increasing levels of sulphate aerosols. *Annales Geophysicae* **16**, 346–353.

Charlson, R. J., Lovelock, J. S., Andreae, M. O. and Warren, S. G. 1987. Oceanic phytoplankton, atmospheric sulphur, cloud albedo and climate. *Nature* **326**, 655–661.

Charlson, R. J., Langner, J., Rodhe, H., Leovy, C. B. and Warren, S. G. 1991. Perturbation of the northern hemisphere radiative balance by backscattering from anthropogenic sulfate aerosols. *Tellus* **43B**, 152–163.

Chin, M., Jacob, D. J., Gardner, G. M., Foreman-Fowler, M. S., Spiro, P. A. and Savoie, D. L. 1996. A global three dimensional model of tropospheric sulphate. *J. Geophys. Res.* **101(D13)**, 18,667–18,690.

Feichter, J., Kjellstrom, E., Rodhe, H., Dentener, F., Lelieveld, J. and Reolofs, G. 1996. Simulation of the tropospheric sulfur cycle in a global climate model. *Atmos. Environ.* **30**, 1693–1707.

Feingold, G., Kreidenweis, S. M. and Zhang, Y. 1998. Statocumulus processing of gases and cloud condensation nuclei (1). Trajectory ensemble model. *J. Geophys. Res.* **103(D16)**, 19,527–19,542.

Gurciullo, C. S. and Pandis, S. N. 1997. Effect of composition variations in cloud droplet populations on aqueous-phase chemistry. *J. Geophys. Res.* **102(D8)**, 9375–9385.

Hegg, D. A. and Larson, T. V. 1990. The effects of microphysical parameterisation on model predictions of sulphate production in clouds. *Tellus* **42B**, 272–284.

Hegg, D. A., Yuen, P.-F. and Larson, T. V. 1992. Modelling the effects of heterogeneous cloud chemistry on the marine particle size distribution. *J. Geophys. Res.* **97 (D12)**, 12,927–12,933.

Hobbs, P. V. 1993. Aerosol-cloud interactions. In: *Aerosol–cloud–climate interactions*, Hobbs, P. V. (ed.). Academic Press: San Diego, CA, pp. 33–69.

Hoffmann, M. R. and Calvert, J. G. 1985. *Chemical transformation modules for Eulerian acid deposition models*, volume 2, *The aqueous phase chemistry*. EPA/600/3–85/017, US Environmental Protection Agency, Research Triangle Park, North Carolina, USA.

Ibusuki, T. and Takeuchi, K. 1987. Sulfur dioxide oxidation by oxygen catalysed by mixtures of manganese(II) and iron(III) in aqueous solutions at environmental reaction conditions. *Atmos. Environ.* **21**, 1555–1560.

Khemani, L. T., Momin, G. A., Rao, P. S.P., Vijaykumar, R. and Safai, P. D. 1995. Study of surface ozone behaviour at urban and forested sites in India. *Atmos. Environ.* **19**, 2021–2024.

Khemani, L. T. 1989. Physical and chemical characteristics of atmospheric aerosols, In: *Encyclopaedia of environmental control technology*, volume 2, P. Cheremisinoff (ed.). Gulf Publishing Company, Houston, pp. 401–453.

Kiehl, J. T. and Briegleb, B. P. 1993. The relative roles of sulfate aerosols and greenhouse gases in climate forcing. *Science*. **260**, 311–314.

Kiehl, J. T. and Rodhe, H. 1995. Modelling geographical and seasonal forcing due to aerosols. In: *Aerosol forcing of climate*, R. J. Charlson and J. Heintzenberg (eds.). Wiley, New York, pp. 281–297.

Kondratyev, K. Ya. 1999. *Climatic effects of aerosols and clouds*. Springer-Praxis: Chichester, UK, 259 pp.

Kosak-Channing, L. F. and Helz, G. R. 1983. Solubility of ozone in aqueous solutions of 0–0.6 M ionic strength at 5–30°C. *Environ. Sci. Technol.* **17**, 145–149.

Kreidenweis, S. M., Zhang, Y. and Taylor, G. R. 1997. The effects of clouds on aerosol and chemical species production and distribution 2. Chemistry model

description and sensitivity analysis. *J. Geophys. Res.* **102(D20)**, 23,867–23,882.

Kulshrestha, U. C., Jain, M., Mandal, T. K., Gupta, P. K., Sarkar, A. K. and Parashar, D. C. 1999. Measurements of acid rain over the Indian ocean and surface atmospheric aerosols at New Delhi during the INDOEX pre-campaign. *Cur. Sci.* **76(7)**, 968–972.

Langner, J. and Rodhe, H. 1991. A global three dimensional model of the tropospheric sulfur cycle. *Atmos. Chem.* **13**, 225–263.

Lelieveld, J., Crutzen, P. J. and Rodhe, H. 1989. *Zonal average cloud characteristics for global atmospheric chemistry modeling*. Report CM-76, Department of Meteorology, University of Stockholm, Sweden.

Mandal, T. K., Kley, D., Smit, H. G. J., Srivastava, S. K., Peshin, S. K. and Mitra, A. P. 1999. Vertical distribution of ozone over the Indian ocean (15 N-20 S) during the first field phase of INDOEX-1998. *Cur. Sci.* **76**, 938–943.

Mitra, A. P. 1999. INDOEX (India). Introductory note. *Cur. Sci.* **76**, 886–889.

Momin, G. A., Rao, P. S.P., Safai, P. D., Ali, K., Naik, M. S. and Pillai, A. G. 1999. Atmospheric aerosol characteristics at Pune and Thiruvanathapuram during the INDOEX programme, 1998. *Cur. Sci.* **76**, 985–989.

Naja, M., Lal, S., Venkataramani, S., Modh, K. S. and Chand, D. 1999. Variabilities in O3, NO, CO and CH4 over the Indian ocean during winter. *Cur. Sci.* **76**, 931–937.

Pandis, S. N. and Seinfeld, J. H. 1989. Sensitivity analysis of a chemical mechanism for aqueous-phase atmospheric chemistry. *J. Geophys. Res.* **94**, 1105–1126.

Pandis, S. N., Russell, L. M. and Seinfeld, J. H. 1994. The relationship between DMS flux and CCN concentration in remote marine regions. *J. Geophys. Res.* **99(D8)**, 16,945–16,957.

Parashar, D. C., Granat, L., Kulshreshtha, U. C., Pillai, A. G., Naik, M. S., Momin, G. A. and Rodhe, H. 1996. *Chemical composition of precipitation in India and Nepal; a preliminary report on an Indo-Swedish project on atmospheric chemistry*. Report CM-90, Department of Meteorology, University of Stockholm, Sweden.

Perrin, D. D. 1982. *Ionisation constants of inorganic acids and bases in aqueous solution.* Pergamon Press, New York.

Pham, M., Muller, J-F., Brasseur, G. P., Granier, C. and Megie, G. 1995. A three dimensional study of the tropospheric sulphur cycle. *J. Geophys. Res.* **100(D12)**, 26,061–26,092.

Pruppacher, R. H. and Klett, J. D. 1997. *Microphysics of clouds and precipitation.* Kluwer Academic Publishers, Boston.

Rao, P. S. P., Momin, G. A., Safai, P. D., Ali, K., Naik, M. S. and Pillai, A. G. 1999. Studies of trace gases and Aitken nuclei at inland and coastal stations — A part of the INDOEX programme. *Cur. Sci.* **76**, 981–984.

Schwartz, S. E. 1986. Mass-transport considerations pertinent to aqueous-phase reactions of gases in liquid-water clouds. In: *Chemistry of multiphase atmospheric systems*, W. Jaeschlke (ed.). Springer, Heidelberg.

Seigneur, C. and Saxena, P. 1984. A study of atmospheric acid formation in different environments. *Atmos. Environ.* **18**, 2109–2124.

Seinfeld, J. H. and Pandis, S. N. 1998. *Atmospheric chemistry and physics: from air pollution to climate change.* Wiley, New York.

Smith, R. M. and Martell, A. E. 1976. *Critical state constants: inorganic complexes.* Plenum Press, New York.

Twohy, C. H., Durkee, P. A., Huebert, B. J. and Charlson, R. J. 1995. Effects of aerosol particles on the microphysics of coastal stratiform clouds. *J. Climate* **8**, 773–783.

Whitby, K. T. 1978. Physical characteristics of sulphur aerosols. *Atmos. Environ.* **12**, 135–159.

Zhang, Y., Kreidenweis, S. M. and Feingold, G. 1999. Stratocumulus processing of gases and cloud condensation nuclei 2. Chemistry sensitivity analysis. *J. Geophys. Res.* **104(D13)**, 16,061–16,080.